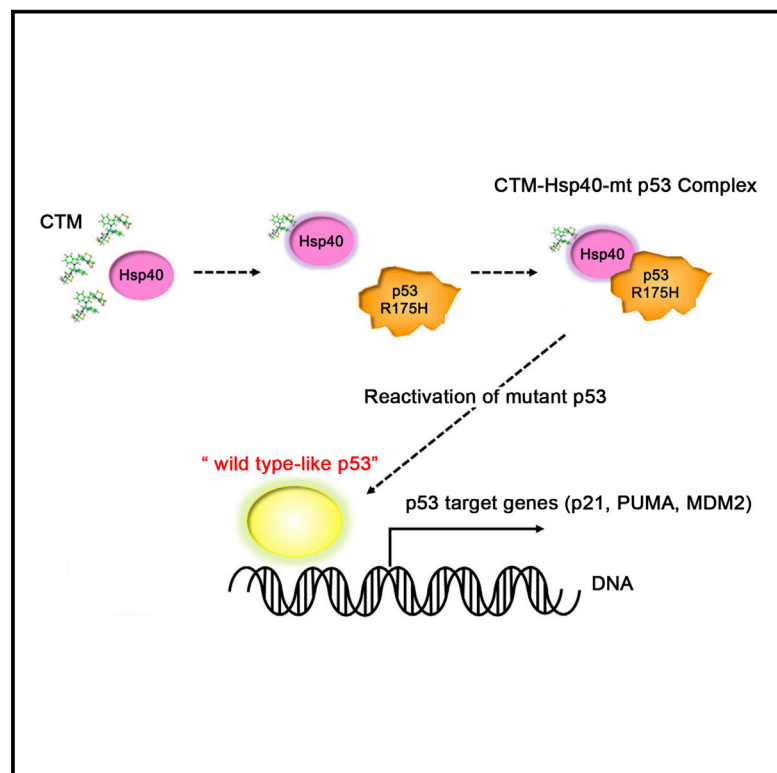


# Chemistry & Biology

## Small-Molecule Reactivation of Mutant p53 to Wild-Type-like p53 through the p53-Hsp40 Regulatory Axis

### Graphical Abstract



### Authors

Masatsugu Hiraki, So-Young Hwang, Shugeng Cao, ..., Anna Mandinova, Jon Clardy, Sam W. Lee

### Correspondence

jon\_clardy@hms.harvard.edu (J.C.), swlee@mgh.harvard.edu (S.W.L.)

### In Brief

Hiraki et al. identified chetomin (CTM) as a mutant p53 R175H reactivator through a cell-based high-throughput small-molecule screening, which enabled transactivation of its target genes, and selectively inhibited the growth of cancer cells with mutant p53 R175H. CTM binding to a chaperone protein Hsp40 caused a potential conformation change of mutant p53 to wild-type-like p53.

### Highlights

- A cell-based small-molecule screen identifies CTM as a mutant p53 R175H reactivator
- CTM inhibits growth of cancer cells harboring mutant p53 R175H in vitro and in vivo
- CTM enables transactivation of p53 targets and restores MDM2 negative regulation
- CTM binds Hsp40, enhances its binding to p53 R175H, and restores WT-like function



# Small-Molecule Reactivation of Mutant p53 to Wild-Type-like p53 through the p53-Hsp40 Regulatory Axis

Masatsugu Hiraki,<sup>1,7</sup> So-Young Hwang,<sup>1,7</sup> Shugeng Cao,<sup>2,3,7</sup> Timothy R. Ramadhar,<sup>3</sup> Sanguine Byun,<sup>1</sup> Kyoung Wan Yoon,<sup>1</sup> Jung Hyun Lee,<sup>1</sup> Kiki Chu,<sup>1</sup> Aditi U. Gurkar,<sup>1</sup> Vihren Kolev,<sup>1</sup> Jianming Zhang,<sup>1</sup> Takushi Namba,<sup>1</sup> Maureen E. Murphy,<sup>4</sup> David J. Newman,<sup>5</sup> Anna Mandinova,<sup>1,6,8</sup> Jon Clardy,<sup>3,8,\*</sup> and Sam W. Lee<sup>1,6,8,\*</sup>

<sup>1</sup>Cutaneous Biology Research Center, Massachusetts General Hospital and Harvard Medical School, Charlestown, MA 02129, USA

<sup>2</sup>Department of Pharmaceutical Sciences, Daniel K. Inouye College of Pharmacy, University of Hawaii at Hilo, 34 Rainbow Drive, Hilo, HI 96720, USA

<sup>3</sup>Department of Biological Chemistry and Molecular Pharmacology, Harvard Medical School, Boston, MA 02115, USA

<sup>4</sup>Program in Molecular and Cellular Oncogenesis, The Wistar Institute, Philadelphia, PA 19104, USA

<sup>5</sup>Natural Products Branch, Developmental Therapeutics Program, Division of Cancer Treatment and Diagnosis, Frederick National Laboratory for Cancer Research, Frederick, MD 21702, USA

<sup>6</sup>Broad Institute of Harvard and MIT, Cambridge, MA 02142, USA

<sup>7</sup>Co-first author

<sup>8</sup>Co-senior author

\*Correspondence: [jon\\_clardy@hms.harvard.edu](mailto:jon_clardy@hms.harvard.edu) (J.C.), [swlee@mgh.harvard.edu](mailto:swlee@mgh.harvard.edu) (S.W.L.)

<http://dx.doi.org/10.1016/j.chembiol.2015.07.016>

## SUMMARY

*TP53* is the most frequently mutated gene in human cancer, and small-molecule reactivation of mutant p53 function represents an important anticancer strategy. A cell-based, high-throughput small-molecule screen identified chetomin (CTM) as a mutant p53 R175H reactivator. CTM enabled p53 to transactivate target genes, restored MDM2 negative regulation, and selectively inhibited the growth of cancer cells harboring mutant p53 R175H in vitro and in vivo. We found that CTM binds to Hsp40 and increases the binding capacity of Hsp40 to the p53 R175H mutant protein, causing a potential conformational change to a wild-type-like p53. Thus, CTM acts as a specific reactivator of the p53 R175H mutant form through Hsp40. These results provide new insights into the mechanism of reactivation of this specific p53 mutant.

## INTRODUCTION

The tumor suppressor p53 is mutated in at least half of human cancers (Joerger and Fersht, 2008; Levine and Oren, 2009). Loss of p53 function plays a pivotal role in the initiation as well as the progression of cancers. Recent large-scale genomics analysis found that some cancer types exhibit very high frequencies of p53 mutation, including ovarian cancer (95%), lung squamous cell carcinoma (84%), head and neck cancer (67%), and esophageal adenocarcinoma (65%) (Lawrence et al., 2014). p53 functions as a transcription factor and is activated in response to various cellular stresses, such as DNA damage, oncogene activation, and hypoxia (Joerger and Fersht, 2008;

Levine and Oren, 2009). Once activated, p53 induces its downstream target genes and promotes cell-cycle arrest, apoptosis, senescence, and DNA repair (Allen et al., 2014; Joerger and Fersht, 2008; Levine and Oren, 2009). Thus, p53 is a tumor suppressor gene and is frequently called the guardian of the genome (Lane, 1992). The majority of clinically useful traditional anticancer drugs includes DNA-damaging agents, and the activities rely on functional wild-type (WT) p53 for anticancer effects. In addition, mutant p53 has a gain-of-function phenotype that promotes more aggressive cancer forms. Thus, cancer cells harboring p53 mutants have been reported to exhibit chemoresistance to many conventional anticancer agents (Muller and Vousden, 2014; Willis et al., 2004). This dramatic dependence on functional p53 argues that restoring p53 function is an important approach for cancer therapy, and several earlier studies have reported targeting mutant p53 using small molecules, peptides, and adenovirus (Chen et al., 2010; Hong et al., 2014; Mandinova and Lee, 2011).

In this study, we have identified a natural compound, chetomin (CTM) from a fungus extract as a novel p53 R175H mutant reactivator in a cell-based, high-throughput screen. We found that CTM restores p53 function, and can transactivate and induce p53 target genes in vitro and in vivo through the p53-heat-shock protein 40 (Hsp40) axis.

## RESULTS

### Identification of CTM as a Mutant p53 R175H Reactivator

To identify small molecules that reactivate mutant p53, a luciferase reporter-based, high-throughput chemical screen against the R175H structural mutant was performed. For the screen, we established a stable cell line with mutant p53 R175H and a luciferase reporter carrying the p53 DNA binding site of the *PUMA* promoter in p53-null H1299 lung cell carcinoma cells

(H1299-mtp53 R175H/PUMA-luc). We first verified the responsiveness of this luciferase reporter cell line by infection with Ad-p53 expressing WT p53, which significantly increased luciferase activity, whereas treatment with Ad-GFP showed no effect (Figure 1A). We then performed high-throughput chemical screening, as outlined in Figure 1B, with a chemical library containing 20,000 compounds and 36,256 natural extracts (from the National Cancer Institute [NCI] Natural Products Repository) to identify compounds that increase luciferase activity of the *PUMA* promoter. Five top hits (#1–5) that consistently showed more than 2.5-fold increased luciferase activity compared with DMSO control were chosen (Figure 1C). All five candidates were from the fungal extract library. We performed validation experiments and found that fungal extracts #4 and #5 showed the strongest effect. Extracts #4 and #5 were effective in inducing *PUMA* promoter activity in a dose-dependent manner (Figures S1A and S1B, top left), and showed significantly higher cytotoxic effects toward mutant p53 R175H cells such as KLE, FAMPAC, SK-BR-3, AU565, and TOV-112D than toward p53 null cells including SK-OV-3, HCT116 p53<sup>-/-</sup>, and H1299 (Figures S1A and S1B, middle left). Although the *p53* gene in the HCT116<sup>-/-</sup> cell line is not fully deleted, it has been reported as a p53-deficient cell line (Bunz et al., 1998; Murray-Zmijewski et al., 2006). In addition, when treated to mouse embryonic fibroblasts (MEFs) expressing one of p53 R172H, R172P (the mouse equivalent to R175 in human), and WT p53, or to p53 null MEFs, extracts #4 and #5 were both able to induce significant cell death only in the mutants p53 R172P and R172H MEFs, unlike the known mutant-p53 reactivator MIRA-1 (Bykov et al., 2005) (Figures S1A and S1B, bottom left). In response to extract #4, mRNA and protein expression levels of p53 target genes such as *p21* and *PUMA* were induced in cancer cell lines that harbor mutant p53 R175H, while there was little effect in cancer cells with WT p53 or in p53 null cells. Extract #5 also showed similar results in protein expression level of p53 target genes (Figures S1A and S1B, right). Based on these results, extracts #4 and #5 were chosen for further investigation.

To identify the active molecule(s) from the natural extracts, we fractionated the extract #4 (fractions 1–7) and #5 (fractions 1–9) by high-performance liquid chromatography (HPLC) (Figure 1D) and tested *PUMA* promoter reporter activity in H1299-mtp53 R175H/PUMA-luc cells. Treatment with fraction 4 of extract #4 or fraction 6 of extract #5, respectively, demonstrated the highest luciferase activity (Figure 1D). We then analyzed these two fractions by nuclear magnetic resonance spectroscopy, and as a result an identical small molecule, chetomin (CTM), was identified from both fractions. CTM is produced by several species in the fungal genus *Chaetomium* (Waksman and Bugie, 1944). The structure of CTM and the 3D image of the CTM global minimum conformation are shown in Figures 1E and 1F, respectively (Table S1). While the relative stereochemistry of CTM is known, its absolute configuration has not been determined. Thus, optical rotation calculations were performed in a similar manner to a previous report (Cherblanc et al., 2011). Through using density functional theory (DFT) with the SCRf(chloroform)-wB97XD/6–311++G(d,p) level of theory (Chai and Head-Gordon, 2008) and assuming the absolute stereochemistry of CTM depicted in Figure 1E, a Boltzmann-weighted optical rotation  $[\alpha]_D^{25} +299^\circ$  was obtained

(Tables S1–S4), which is of the same sign and similar magnitude as the experimental optical rotation for CTM ( $[\alpha]_D^{25} +278^\circ$  CHCl<sub>3</sub>) (Fujimoto et al., 2004). Therefore, the CTM absolute stereochemistry shown in Figure 1E is predicted to be correct. To confirm that CTM is the molecule responsible for the activities of extracts #4 and #5, we tested the effects of purified commercial CTM on the *PUMA* promoter activity in H1299-mtp53 R175H/PUMA-luc cells. As a result, CTM indeed increased *PUMA* promoter activity in a dose-dependent manner (Figure 1G). Meanwhile, it did not show any effect on *NF-κB* luciferase activity (Figure S1C). These results suggest that CTM is a strong candidate small molecule capable of restoring p53 activity from mutant p53 R175H.

### Anticancer Effects and Induction of p53 Target Genes by CTM in Cancer Cell Lines Expressing R175H p53 Mutant

To investigate the anticancer activity of CTM, we treated human tumor cell lines of different p53 statuses including mutant p53 R175H (structural mutation), p53 R273H (contact mutation), WT p53, and p53 null, as well as normal cells. CTM exhibited a higher cytotoxicity to the mutant p53 R175H cell lines than toward mutant p53 R273H, WT p53, or p53 null cell lines (Figure 2A). In mutant p53 R175H cells, such as CAL-33, HuCCT1, FAMPAC, KLE, and TOV-112D, mRNA expression of p53 target genes such as *p21*, *PUMA*, and *MDM2* was significantly induced upon CTM treatment. In fact, the level of induction was comparable with that observed in WT p53 containing positive control HCT116 cells treated with etoposide (ETO) (Figure 2B). Meanwhile, the mRNA expression level of these genes showed little response to CTM in HCT116 (WT), H1299 (null), and PANC-1 (R273H) cells (Figure 2B). CTM also significantly increased protein expression levels of p21 and PUMA in a dose-dependent manner in mutant p53 R175H cells, such as CAL-33, HuCCT1, FAMPAC, and KLE (Figure 2C), whereas slight or no induction was observed in OVCAR-3 (R248Q), A431 (R273H), HCT116 (WT), MCF7 (WT), H1299 (null), and HCT116 p53<sup>-/-</sup> (null) cells (Figure 2D). These results suggest that CTM exerts an anticancer effect with higher specificity toward cancer cells harboring mutant p53 R175H.

### CTM Specifically Targets Mutant p53 R175H and Restores p53 WT-like Properties

To confirm the specificity of CTM to mutant p53 R175H, we knocked down mutant p53 R175H by siRNA and observed at the protein level that the induction of p53 target genes *p21*, *PUMA*, and *Noxa* in response to CTM was impaired in R175H cells, including TOV-112D, KLE, and CAL-33 (Figure 3A, top). A similar result was also observed when p53 was knocked down by short hairpin RNA (shRNA) in FAMPAC (R175H) cells (Figure S2A). In contrast, introduction of mutant p53 R175H to p53 null cells (H1299 and HCT116 p53<sup>-/-</sup>) resulted in induction of p21 and PUMA at the protein level upon CTM treatment, while induction of p21 or PUMA was not observed when mutant p53 R273H was introduced into HCT116 p53<sup>-/-</sup> cells (Figure 3A, bottom). Taken together, these results demonstrate that CTM induces p53 target genes in a mutant p53 R175H-dependent manner.

We next investigated whether CTM restores DNA binding activity of mutant p53 R175H protein by chromatin immunoprecipitation (ChIP) assay. HCT116 cells containing WT p53

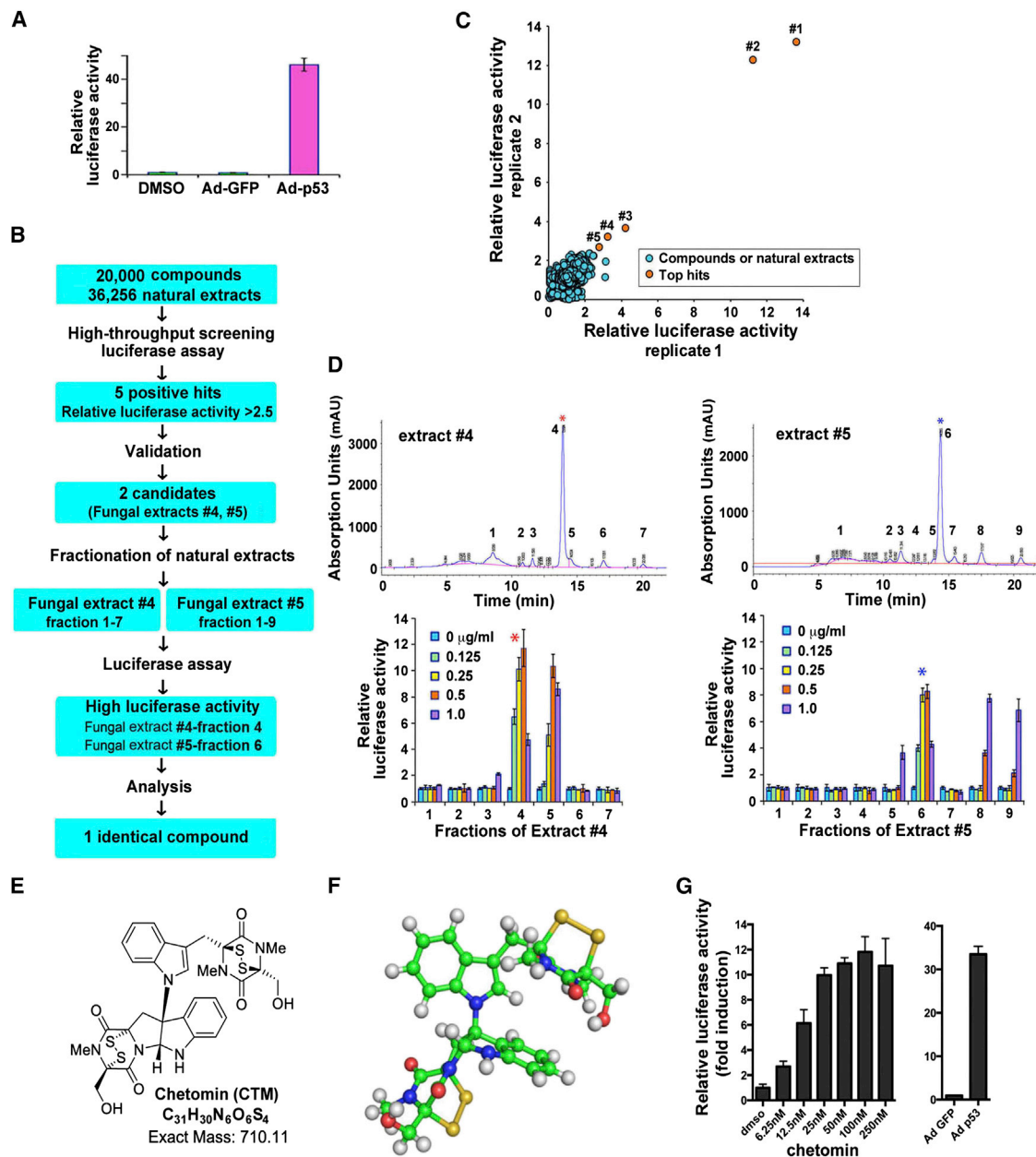


**Figure 1. Identification of CTM as a Mutant p53 R175H Reactivator**

(A) H1299-mutant p53 R175H cells with luciferase reporter carrying the p53 DNA binding site of *PUMA* promoter was generated and tested for luciferase activity with adenovirus (Ad)-GFP or -p53. Data shown are means  $\pm$  SD in triplicate and measured at the same time.

(B) Screening strategy used in this study.

(C) High-throughput chemical screening was performed in duplicate, and relative luciferase activity calculated.

(D) Fractionation of natural extracts #4 and #5 by HPLC methods, and luciferase activity assays of resulting fractions of natural extracts. Each natural extract was subjected to HPLC fractionation (#4, fractions 1–7; #5, fractions 1–9). Each fraction from extracts #4 and #5 was analyzed by luciferase assay using H1299-mutant p53 R175H cells with luciferase reporter carrying the p53 DNA binding site of *PUMA* promoter. Cells were treated with each fraction at indicated concentrations for 15 hr. Luciferase activity was then measured. Asterisks indicate the fractions that exhibited the highest luciferase activity. Data shown are mean  $\pm$  SD in triplicate and measured at the same time.

(E) Chemical structure of chetomin with absolute stereochemistry predicted through optical rotation calculations.

(F) Global minimum conformation of chetomin calculated using DFT at the SCRf(chloroform)-wB97XD/6-311++G(d,p) level of theory. See also Table S1.

(G) CTM was analyzed by luciferase assay using H1299-mutant p53 R175H cells with luciferase reporter carrying the p53 DNA binding site of *PUMA* promoter. Cells were treated with CTM at indicated concentrations for 15 hr, after which luciferase activity was measured. Data shown are mean  $\pm$  SD in triplicate and measured at the same time. Adenoviruses Ad-GFP and Ad-p53 were used as negative and positive controls for luciferase assay, respectively. See also Figure S1.

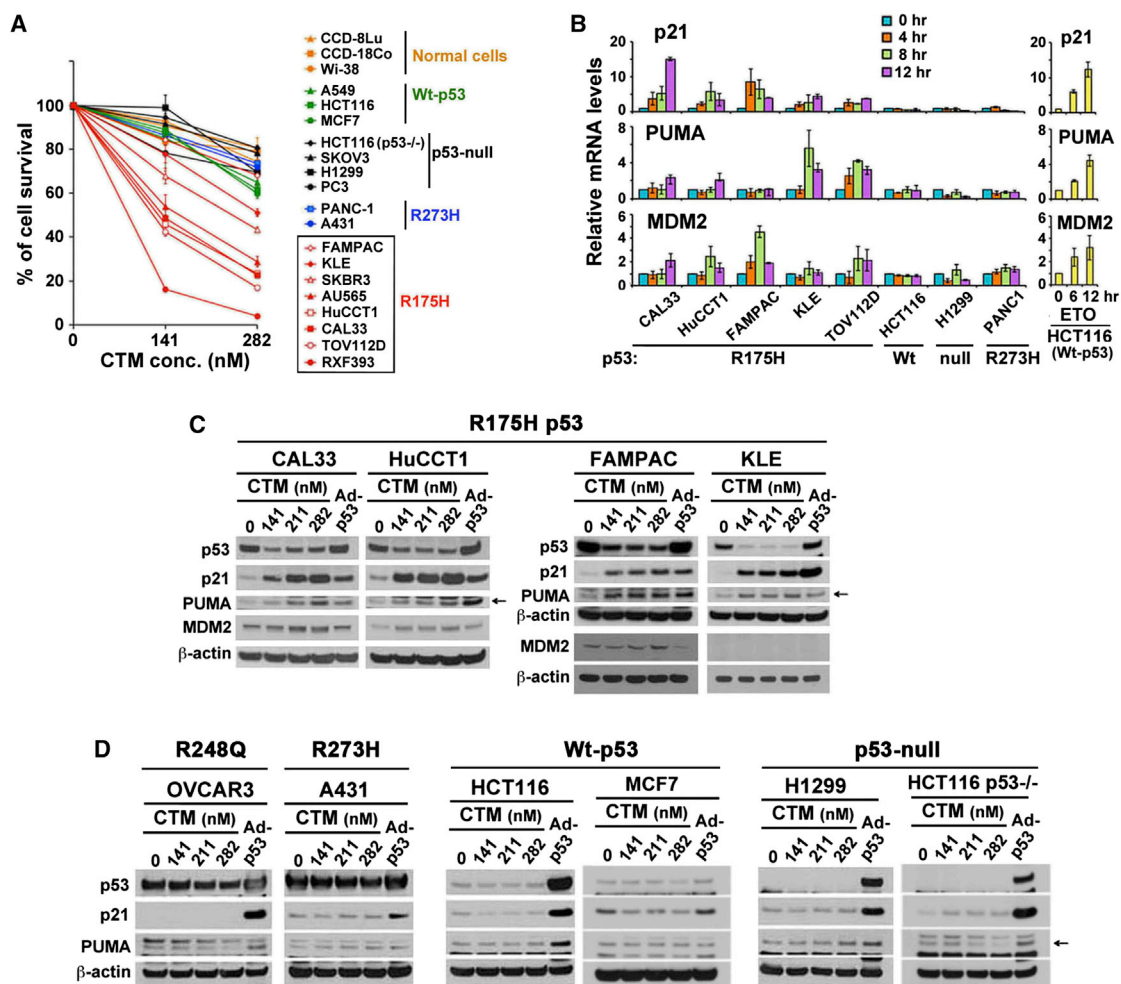


**Figure 2. CTM Preferentially Suppresses Cancer Cells with p53 R175H and Induces p53 Target Genes**

(A) CTM shows high anticancer activity in mutant p53 R175H cells. Normal and cancer cells including p53 WT, p53 null, mutant p53 R175H, and R273H were treated with CTM for 24 hr at indicated concentrations. Cells were stained with sulforhodamine B and measured for cell viability. Error bars represent the range of duplicates.

(B) p53 target genes are highly induced in mutant p53 R175H cells. Cancer cells (R175H: CAL-33, HuCCT1, FAMPAC, KLE, and TOV-112D; WT: HCT116; null: H1299; R273H: PANC-1) with various statuses of p53 were treated with CTM (150 nM) for indicated times. Total RNA was extracted and subjected to quantitative real-time PCR with specific primers for *p21*, *PUMA*, and *MDM2*. HCT116 cells were treated with etoposide (50  $\mu$ M) for indicated time points as a positive control. Data shown are mean  $\pm$  SD in triplicates and measured at the same time.

(C and D) CTM-mediated p53 target protein induction in mutant p53 R175H cells. Cancer cells (R175H: CAL-33, HuCCT1, FAMPAC, and KLE; R248Q: OVCAR-3; R273H: A431; WT: HCT116; null: H1299) with various statuses of p53 were treated with CTM for 18 hr, and cell lysates were analyzed by western blotting with indicated antibodies. Arrows mark the band corresponding to PUMA. Ad-p53 was used as a positive control.

showed significant p53 occupancy at *p21*, *PUMA*, and *MDM2* promoters in response to the DNA-damaging reagent ETO, while CTM showed little effect (Figure 3B). However, H1299 cells transfected with mutant p53 R175H and CAL-33 (R175H) cells showed increased p53 promoter occupancy at *p21*, *PUMA*, and *MDM2* promoters upon CTM treatment. To test whether this was due to a CTM-specific effect, ETO was treated and the occupancy of mutant p53 examined through ChIP assay in H1299 cells transfected with mutant p53 R175H. As a result, ETO treatment showed little effect on mutant p53 occupancy, corroborating the importance of chetomin as a mutant p53-specific compound (Figure S2B). Thus, it appears that CTM can restore DNA binding activity of mutant p53 R175H protein.

Notably, we observed that upon CTM treatment, the p53 protein level significantly decreased in mutant p53 R175H cells while remaining relatively stable in OVCAR-3 (R248Q) and A431 (R273H) cells (Figures 2C and 2D). Based on this finding, we came to suspect that the restoration of WT p53 function by CTM might have resulted in increased negative regulation by MDM2, leading to decreased level of the mutant p53 R175H protein. To test this idea, we assessed the impact of MDM2 negative regulation on CTM-treated mutant p53 R175H using Nutlin-3, a well-known MDM2 antagonist. Nutlin-3 treatment alone did not affect p53 protein level, whereas CTM treatment alone resulted in a decrease in p53 level in mutant p53 R175H cells (CAL-33, KLE, HuCCT1, and FAMPAC), but not in A431 (R273H) and OVCAR-3

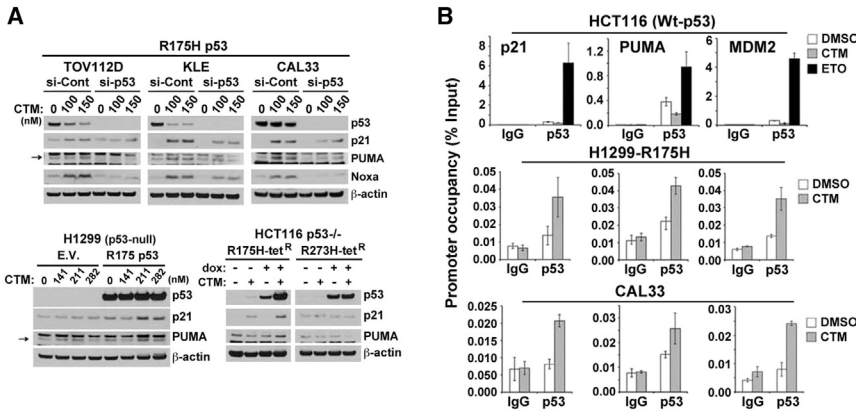


**Figure 3. Mutant p53 Reactivation Effect of CTM Is Mediated through p53 R175H**

(A) Knockdown of mutant p53 R175H impairs induction of p53 target genes by CTM. Cells were transfected with siRNA (si control or sip53) and treated with CTM for 18 hr. Overexpression of mutant p53 R175H increased the protein expression level of p53 target genes. H1299 (p53-null) cells were transfected with pcDNA3-empty or mutant p53 R175H plasmid. Stable cells were treated with CTM for 18 hr. HCT116 p53<sup>-/-</sup> cells overexpressing mutant p53 R175H or R273H by tetracycline-inducible system were treated with CTM (150 nM) for 18 hr. Mutant p53 was overexpressed by doxycycline for 48 hr prior to CTM treatment.

(B) ChIP analysis shows that CTM treatment restores the transactivation function of p53 in

mutant p53 R175H cells. Cells were treated with DMSO, etoposide (50  $\mu$ M), or CTM (200 nM) and cross-linked. Sheared chromatin was immunoprecipitated with p53 antibody. Eluted DNA was examined by quantitative real-time PCR using primers that specifically target p53 binding site in the promoter. Data shown are mean  $\pm$  SD in triplicate. See also Figure S2.

(R248Q) cells. However, when p53 R175H cells (CAL-33, KLE, HuCCT1, and FAMPAC) were treated with both Nutlin-3 and CTM, the decrease in p53 was inhibited (Figures 4A and S3A). We also observed that MDM2 protein level was induced upon CTM treatment, and the binding between mutant p53 and MDM2 protein was significantly increased upon CTM treatment but inhibited upon addition of Nutlin-3 in CAL-33 cells (Figure 4B). Furthermore, to examine whether co-treatment of Nutlin-3 and CTM, which appears to lead to stabilization of functionally restored p53 R175H, might result in synergistic effects on p53 target gene induction, we checked mRNA levels of p53 target genes through quantitative real-time PCR assay in HuCCT1 cells and CAL-33 cells treated with either CTM or Nutlin-3 alone, or with both CTM and Nutlin-3. As a result, while Nutlin-3 alone did not cause an increase, co-treatment of Nutlin-3 and CTM resulted in increased levels of mRNA, demonstrating additive or synergistic effects in a gene-dependent manner (Figure S3B). These results indicate that CTM restores mutant p53 R175H function to WT-like p53, thus activating the induction of MDM2, which then binds to and negatively regulates p53 R175H.

**Antitumor Effect of CTM in Xenograft Tumor Model**

To investigate whether CTM can reactivate the mutant p53 R175H in vivo, mouse xenografts of various tumor cell lines carrying mutant p53 R175H, p53 R273H, or p53 null were generated. In mutant p53 R175H-carrying TOV-112D and CAL-33 tumors, CTM treatment resulted in significant reduction of tumor volume (up to 71% and 59% at end point, respectively) and weight (71% and 51% at end point, respectively) (Figure 5A). However, CTM did not inhibit in vivo tumor growth of A431 (R273H) (Figure 5B) and H1299 (p53 null) (Figure 5C) tumors. These findings further support the idea that the antitumor effect of CTM is specific to the p53 R175H mutation.

**Hsp40 Is a CTM Target and Mediator of Mutant p53 R175H Reactivation**

To explore the mechanism by which CTM affects mutant p53 R175H, we investigated whether CTM could directly bind to mutant p53 R175H protein. However, in a gel-shift assay to assess DNA binding activity of mutant p53 R175H upon CTM treatment, no increase in direct DNA binding ability was

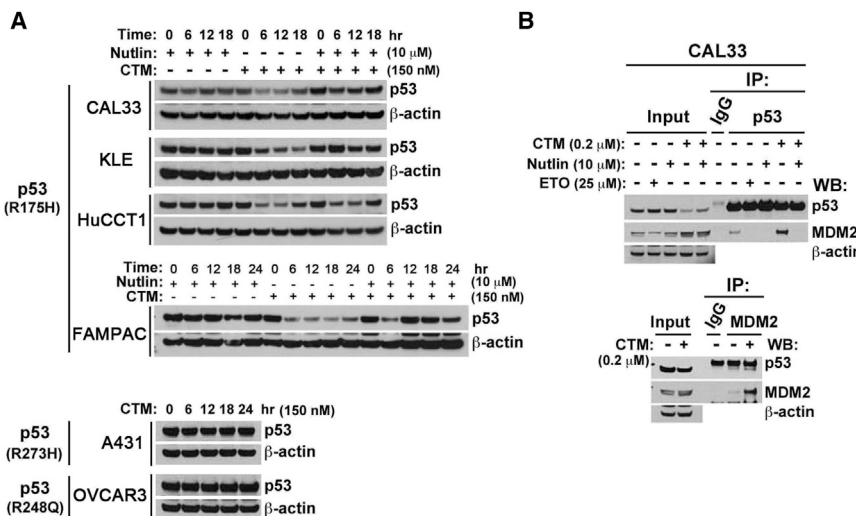


**Figure 4. CTM Restores p53 WT-like Properties in Mutant p53 R175H**

(A) p53 level is decreased upon CTM treatment due to MDM2-negative regulation in mutant p53 R175H cells, but not in mutant p53 R275H and R248Q cells. Cells were treated with Nutlin-3 and/or CTM at indicated concentrations and time.

(B) CTM treatment increased MDM2 protein level and binding capacity to p53 protein in R175H cells. Cells were treated with etoposide, CTM, and/or Nutlin-3 as described, and co-immunoprecipitation was performed with cell lysate using anti-p53 or -MDM2 antibody. Input and co-immunoprecipitate (IP) were analyzed with indicated antibodies. See also Figure S3.

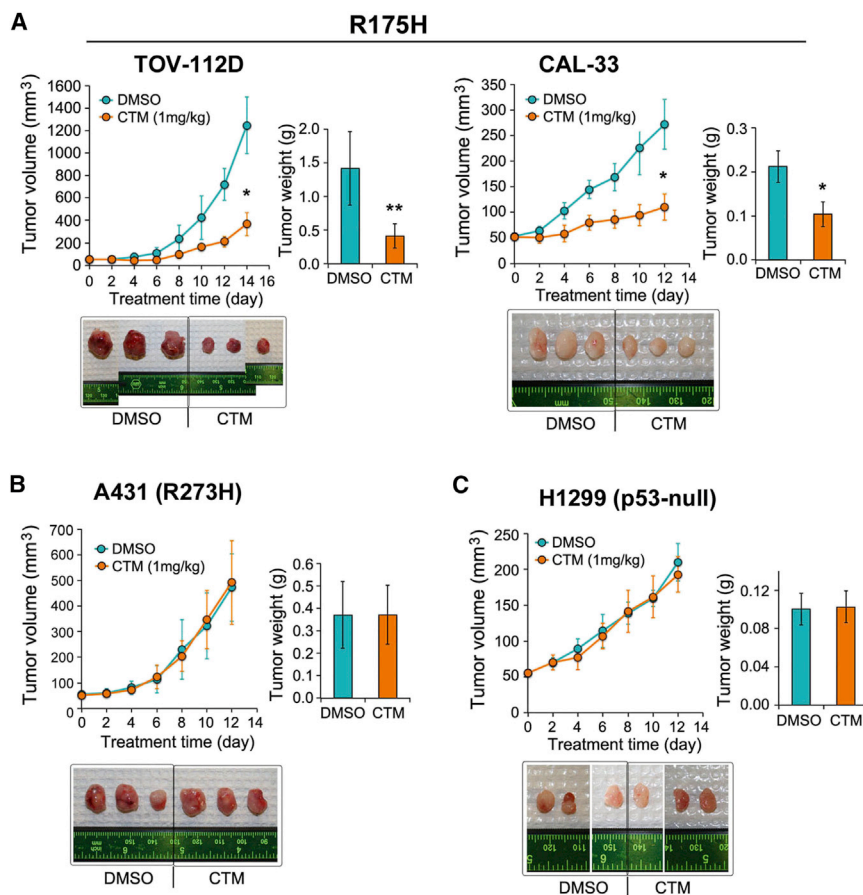


**Figure 5. CTM Suppresses Tumor Growth In Vivo in a p53 R175H Mutant-Dependent Manner**

(A–C) Various types of p53 cells were used for xenograft model: (A) TOV-112D (p53-R175H) and CAL-33 (p53-R175H); (B) A431 (p53-R273H); and (C) H1299 (p53-null). Tumors were allowed to grow to 50 mm<sup>3</sup> before intraperitoneal injection of DMSO or CTM at 1 mg/kg/day for indicated days. Tumor volume and weight were measured. Numbers of mice examined are as follows: TOV-112D (DMSO control: n = 7 and CTM-treated: n = 6), CAL-33 (DMSO control: n = 9 and CTM-treated: n = 9), A431 (DMSO control: n = 6 and CTM-treated: n = 6), H1299 (DMSO control: n = 8 and CTM-treated: n = 8). Data shown are mean ± SD. Student's t test: \*p < 0.001, \*\*p < 0.005.

observed (Figures S4A and S4B). This suggests that CTM does not bind to or directly affect the mutant p53 R175H protein. Thus, we investigated potential CTM binding partners with a co-immunoprecipitation-coupled mass spectrometry analysis to identify the direct targets of CTM (Figure S4C). Mass spectrometry data demonstrated that most known p53 binding partners were decreased in unique peptide number upon CTM treatment, a finding in accordance with the previously observed decrease in p53 protein level (Table S5) (Avantaggiati et al., 1997; Bates et al., 2005; Gaiddon et al., 2001; Lee et al., 2002; Yuan et al., 2010). However, upon CTM treatment, some p53 binding partners such as YBX1, WDR33, and Hsp40 homolog (DNAJC8) showed increased binding to p53 (King et al., 2001; Okamoto et al., 2000; Stelzl et al., 2005).

As previously reported, heat-shock proteins, which have been identified as p53 binding partners, function as chaperone or co-chaperone proteins to regulate protein conformation and stability (King et al., 2001; Rosser and Cyr, 2007; Sugito et al., 1995). Therefore, we focused on the role of Hsp40 in reactivation of mutant p53 R175H upon CTM treatment. Consistent with the mass spectrometry data, only Hsp40, but not Hsp90, showed increased binding affinity to mutant p53 upon CTM treatment (Figure 6A). The induction of Hsp40 protein was observed only upon CTM treatment and not in response to treatments with known DNA-damaging agents (ETO and camptothecin) or the known mutant p53 reactivators (MIRA-1 [Bykov et al., 2005]

and PRIMA-1 [Bykov et al., 2002]) (Figure S4D). Notably, knockdown of Hsp40 by siRNA impaired the protein level induction of p53 target genes upon CTM treatment (Figure 6B). We also observed that CTM enhanced Hsp40 binding to mutant p53 R175H protein in a dose-dependent manner in an in vitro binding assay using recombinant proteins (Figure 6C, top), which was not seen with PRIMA-1 or MIRA-1 (Figure S4E). Interestingly, this in vitro binding assay also showed that upon CTM addition, p53-R175H/Hsp40 complex was detected by WT-specific antibody PAb1620 (Figure 6C, bottom). Intrigued by these observations, we next determined the effects of CTM on the DNA binding activity of p53 R175H in the presence of Hsp40. When using purified recombinant Hsp40 and mutant p53-DBD-R175H for gel-shift assay, CTM showed little effect. However, when the nuclear extract of TOV-112D (R175H) cell was used to repeat this experiment, CTM treatment increased the DNA binding activity of p53-DBD-R175H (Figure S5). As another approach, using a Biacore assay, we confirmed that CTM binds to Hsp40 with a  $K_D$  value of 3.7  $\mu$ M based on surface plasmon resonance data analysis (Figures 6D and S6A). Next, the binding affinity of CTM toward Hsp40 and p53 R175H was examined. Varying concentrations of CTM were injected in addition to Hsp40 over immobilized p53R175H. Although the addition of CTM resulted in a slight increase of binding affinity between Hsp40 and p53 R175H, the level of increase was not sufficient to determine the  $K_D$  toward this complex (Figure S6B). This observation is consistent with the aforementioned gel-shift assay results, where little effect of CTM was observed when testing with purified Hsp40 and p53 R175H proteins. The positive gel-shift assay result obtained when using nuclear extract of TOV-112D (R175H) cell (Figure S5) implies the involvement of a yet unidentified factor(s) present in vivo that contributes to the higher potency of CTM in vivo. Binding of CTM to mutant p53 R175H and Hsp70 were also tested, but no significant interaction was detected. In addition, no interaction was detected between

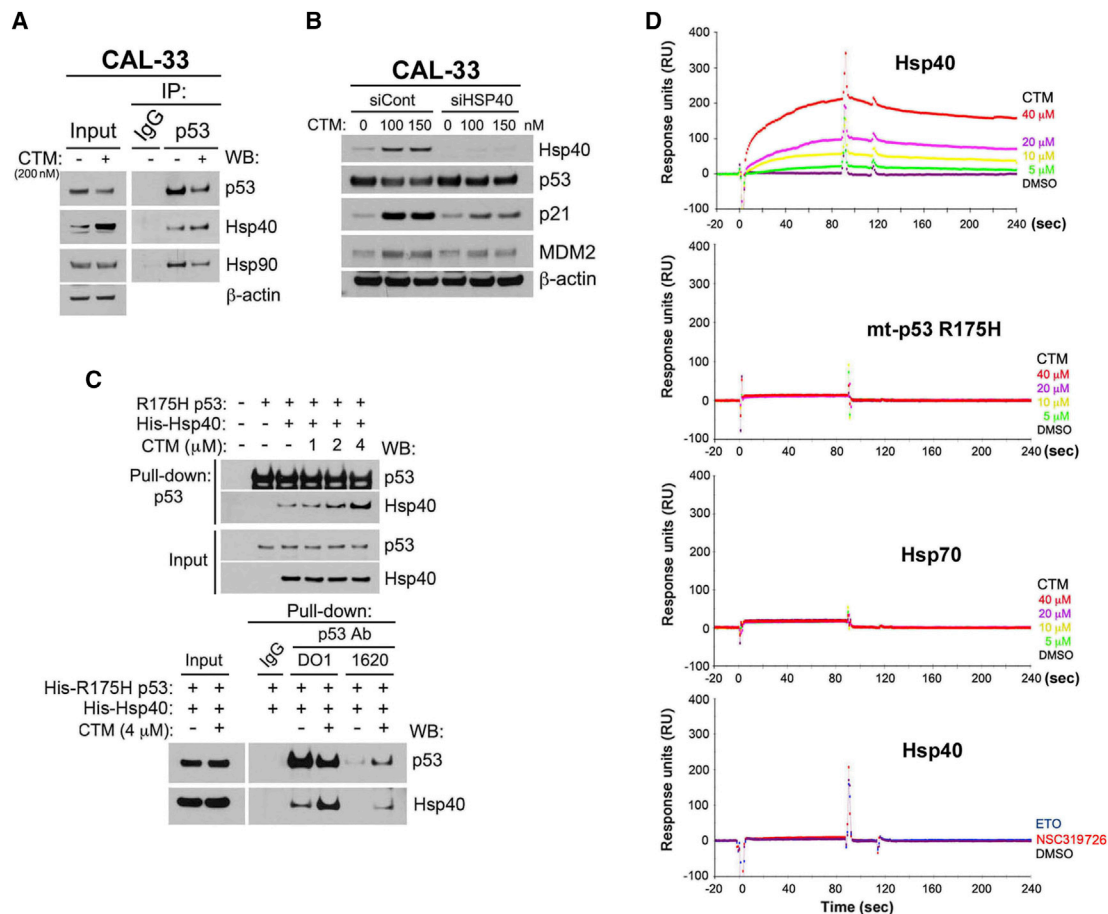


**Figure 6. Binding of CTM to the Hsp40 Protein Is Required for the CTM-Mediated Reactivation of Mutant p53 R175H**

(A) Hsp40 expression is increased and its binding capacity to mutant p53 is enhanced upon CTM treatment in CAL-33 (R175H) cells. Cells were treated with CTM (200 nM) for 8 hr and co-immunoprecipitation was performed with cell lysate using anti-p53 antibody. Input and co-IP were analyzed with indicated antibodies. (B) Hsp40 depletion impairs protein induction of p53 target genes upon chetomin treatment. CAL-33 cells were transfected with siRNA (si control and si-p53) and treated with CTM for 18 hr. Cell lysates were analyzed by western blotting. (C) CTM treatment increases the binding capacity of Hsp40 protein to mutant p53 R175H *in vitro*. Top: Recombinant proteins of mutant p53 R175H (250 nM) and His-Hsp40 (1  $\mu$ M) were incubated with or without CTM at increasing concentrations (1, 2, and 4  $\mu$ M), and pull-down assays were performed with anti-p53 antibody DO1, which recognizes both WT and mutant p53. Bottom: Recombinant proteins of His-mutant p53 R175H (55 nM) and His-Hsp40 (1  $\mu$ M) were incubated with or without CTM (4  $\mu$ M), and pull-down assays were performed with either anti-p53 antibody DO1 or anti-p53 antibody PAb1620 (WT specific). (D) CTM binds to Hsp40 in a concentration-dependent manner. Physical interaction between CTM and Hsp40, mt-p53 R175H, or Hsp70 was tested through Biacore assay. A 2-fold dilution series of CTM, ranging from 0 to 40  $\mu$ M, was tested for binding. In addition, physical interaction between Hsp40 and either NSC319726 (40  $\mu$ M) or etoposide (40  $\mu$ M) was tested through Biacore assay. Each series of experiments was tested in duplicate. See also [Figures S4–S6](#) and [Table S5](#).

Hsp40 and other small molecules such as ETO or NSC319726, a previously reported reactivator of mutant p53 R175H (Yu et al., 2012) (Figure 6D). These results corroborate the specificity of CTM toward Hsp40 and p53 R175H in the process of reactivating p53 R175H.

## DISCUSSION

Several small molecules, including PRIMA-1, MIRA-1, and CP-31398, have been reported as mutant p53 reactivators (Bykov et al., 2002, 2005; Foster et al., 1999). However, only PRIMA-1<sup>MET</sup> (PRIMA-1 analog), also known as APR-246, is currently in clinical trials (phase Ib, NCT02098343) and has a

report on a completed phase I study (Hoe et al., 2014). Thus, discovering small molecules that restore function to mutant p53 remains an important research goal for generating drug leads and developing new therapeutics. Mutant p53 has several hot-spot mutations, categorized into two classes: contact mutations and structural mutations (Bullock and Fersht, 2001; Joerger and Fersht, 2008). While either type results in the loss of p53 transactivation function, contact mutations, such as R248 and R273, directly inhibit the ability of p53 to bind DNA, while structural mutations, such as R175, alter the conformation of p53 protein to abrogate DNA binding.

Recently, two compounds, NSC319726 (Yu et al., 2012) and stictic acid (Wassman et al., 2013), were reported as mutant



p53 reactivators. The mechanism of mutant p53 R175H reactivation by NSC319726 was reported to be through its zinc ion-chelating and redox-changing function. Stictic acid (Wassman et al., 2013) was identified through an ensemble-based virtual screening approach, and its mechanism of reactivation is through docking of the small molecule in the open L1/S3 p53 binding pocket around Cys124, Cys135, and Cys141. These two reports indicate multiple mechanisms for reactivating mutant p53. We also focused on the structural mutant p53 R175H with an intact DNA binding site over contact mutants, as the likelihood of finding a small molecule effecting a p53 conformational change back to WT seemed higher than correcting a contact mutant with lost DNA binding ability. In addition, among the various hot-spot mutations, R175H is the most frequent (Leroy et al., 2013).

In this study we examined 20,000 chemical compounds and 36,256 natural product extracts, and identified CTM through cell-based screening using a luciferase reporter assay. CTM indeed induced p53 target genes such as *p21*, *PUMA*, and *MDM2*, and showed anticancer effects in an R175H-specific manner in vitro and in vivo. Moreover, its ability to induce MDM2 resulted in increased p53-MDM2 binding and p53 degradation, which was inhibited by Nutlin-3. CTM also increased p53 occupancy on p53 target promoter binding sites in mutant p53 R175H cells. The conformational change of the mutant p53 R175H to WT was shown by its increased detection by WT p53-specific antibody, PAb1620. Collectively, these results strongly suggest that CTM can reactivate mutant p53 and restore it to WT-like function, including restoration of MDM2 negative regulation.

We observed that R175H mutant-harboring cell lines are in general more sensitive to CTM than cell lines with R273H mutant or WT p53 (Figure 2A). In addition, among different R175H mutant cells there was a different degree of sensitivity to CTM, suggesting that there may be more factors other than R175H mutation contributing to the sensitivity toward CTM, although further details remain to be elucidated. For instance, it was previously reported that CTM exerts antitumor activity through targeting the interactions between HIF-1 $\alpha$  and p300 (Kessler et al., 2010; Kung et al., 2004; Staab et al., 2007) in conditions whereby HIF-1 $\alpha$  is stabilized. Although our experiments were not carried out in such conditions, and thus argues against this possibility, we still cannot exclude the possibility of other factors contributing to the antitumor effects of CTM observed in our settings. CTM is a member of the epidithiodiketopiperazine family of natural products. Chaetocin, another member of this family, has been previously reported to show activities similar to those of CTM in targeting HIF-1 $\alpha$  and p300 interaction (Cook et al., 2009). When we tested the effects of chaetocin, we observed effects similar to those of CTM on p53 R175H destabilization and *p21* gene induction in p53 R175H-harboring cells (Figure S6C). This result demonstrates the value of CTM as a lead compound.

The mechanism by which CTM reactivates mutant p53 R175H does not appear to involve direct binding between CTM and p53 R175H protein. However, mass spectrometry results suggested Hsp40 as a promising target of CTM, a possibility further supported by previous reports showing that Hsp40 can bind to WT and mutant p53 proteins and act as a chaperone to stabilize unfolded p53 proteins (King et al., 2001; Rosser and Cyr, 2007;

Sugito et al., 1995). We demonstrated that CTM increases the binding of Hsp40 to mutant p53 R175H upon treatment, and that reactivation of mutant p53 R175H is suppressed by knock-down of Hsp40. We also confirmed through Biacore assay that CTM directly binds Hsp40 protein and that the CTM-Hsp40-p53 R175H in vivo complex can be recognized by the WT p53-specific antibody PAb1620. All of these findings indicate that CTM-Hsp40 functions to revert mutant p53 R175H to WT-like conformation. Previous studies have described other small molecules that reactivated mutant p53 through heat-shock proteins. PRIMA-1 treatment resulted in translocation of Hsp90 $\alpha$  to the nucleus, and enhanced binding between Hsp90 $\alpha$  and mutant p53 (Rehman et al., 2005). Similarly, its analog PRIMA-1<sup>MET</sup> is reported to induce Hsp70 and co-localization with mutant p53 in the nucleoli (Rokaeus et al., 2007). Thus, these studies support a role for heat-shock proteins in the refolding and reactivation of mutant p53 protein.

In conclusion, this study shows that CTM can restore mutant p53 R175H to WT-like p53 function through direct interaction and activation of Hsp40, demonstrating the critical role of Hsp40 in reactivating mutant p53 R175H in cancer cells, and providing novel insights into mutant p53 R175H reactivation.

## SIGNIFICANCE

**TP53 gene is mutated in more than 50% of human cancers, including ovarian cancer, head and neck cancer, and lung cancer. Among the most frequently found mutations is R175H, which alters the conformation of p53 and disrupts its negative regulation, as well as target gene induction, thus promoting tumorigenesis. Therefore, pharmacologically restoring mutant p53 R175H to WT activity is anticipated to be an effective strategy for targeting cancer. Here we report CTM as a novel reactivator of mutant p53 R175H identified by high-throughput, cell-based screening of chemical compounds and natural product libraries. CTM restores DNA binding activity of mutant p53 R175H, and also restores MDM2-mediated negative regulation of mutant p53 R175H. Furthermore, our findings suggest that the mechanism of action of chetomin requires interaction with Hsp40. Therefore, we not only report a lead compound for mutant p53 reactivator drug discovery, but also present a novel approach that involves heat-shock protein in restoring mutant p53 function for anticancer therapeutics.**

## EXPERIMENTAL PROCEDURES

### Cell Lines and Culture Conditions

Cells were cultured in media containing 10% fetal bovine serum (Gibco), 100 U/ml penicillin, and 10  $\mu$ g/ml streptomycin at 37°C. DMEM (Cellgro) was used for FAMPAC (human pancreatic cancer cells), HCT116 p53<sup>+/+</sup> (human colorectal cancer cells), HCT116 p53<sup>-/-</sup> (human colorectal cancer cells), SK-OV-3 (human ovarian cancer cells), H1299 (human lung cancer cells), PC3 (human prostate cancer cells), PANC-1 (human pancreatic cancer cells), A431 (human epidermoid carcinoma cells), A549 (human lung cancer cells), MCF7 (human breast cancer cells), and TOV-112D (human ovarian cancer cells). DMEM/F12 (Cellgro) medium was used for CAL-33 (human tongue cancer cells), KLE (human endometrial cancer cells), and SK-BR-3 (human breast cancer cells). RPMI 1640 (Cellgro) was used for AU-565 (human breast cancer cells), HuCCT1 (human bile duct cancer cells), and RXF393 (human renal cell carcinoma). MEM (Cellgro) was used for CCD-8Lu (lung fibroblast), WI-38

(lung fibroblast), and CCD-18Co (colon fibroblast). Various p53 statuses of MEFs (WT p53, R172P, R172H, and p53 null) were kindly provided by Z. Yuan (Harvard School of Public Health). The HCT116 p53<sup>-/-</sup> with tetracycline-inducible mutant p53-R175H and -R273H were gifts from X. Chen (University of California, Davis). p53 statuses of the cell lines were previously reported in reference websites (<http://p53.free.fr/>, <http://www-p53.iarc.fr>, and [http://cancer.sanger.ac.uk/cancergenome/projects/cell\\_lines/](http://cancer.sanger.ac.uk/cancergenome/projects/cell_lines/)) or confirmed as previously documented (Sjogren et al., 1996).

### Plasmids and Adenovirus Constructs

The pcDNA3-Flag-HA mutant p53 R175H plasmid was kindly provided by X. Chen (University of California, Davis). p53-Expressing adenovirus (Ad-p53) and GFP-expressing adenovirus (Ad-GFP) were generated as previously reported (He et al., 1998). For the *PUMA*-Luc reporter plasmid, p53 binding site of the *PUMA* promoter in a plasmid obtained from J. Manfredi (originally from Lin Zhang) was subcloned into pGL4.20-Luc vector (Yu et al., 2001).

### Screening

H1299 cells were transfected with pcDNA3-Flag-HA mutant p53 R175H and luciferase reporter plasmid pGL4.20-*PUMA*-luc carrying the p53 responsive element of human *PUMA* promoter to establish a stable cell line, H1299-mtp53 R175H/*PUMA*-luc cells. High-throughput chemical screening was performed as previously described with modifications (Raj et al., 2011). Cells were plated in 25  $\mu$ l of medium containing 9,000 cells per well into a 384-well plate using an automated plate filler. Twenty-four hours after plating, 20,000 small molecules (compound library from Chembridge) or 36,256 natural extracts (from the NCI Natural Products Repository) were pin-transferred from stock plates to the 384-well assay plates containing cells. The final concentration of small molecule and natural extract were 10  $\mu$ M and 1  $\mu$ g/ml, respectively. The assay plates were incubated with compounds or natural extracts for 15 hr, and luciferase activities were measured using 25  $\mu$ l of luciferase assay reagent (Steady-Glo Luciferase Assay System; Promega). Luminescence was measured with an automated plate reader after shaking the assay plate at room temperature for 3 min to allow full signal generation from the lysed cells. All small molecules and natural extracts were tested in duplicate.

### Chemicals

The following chemicals were purchased and dissolved in DMSO: CTM (Sigma-Aldrich), etoposide (Sigma-Aldrich), camptothecin (Sigma-Aldrich), PRIMA-1 (Sigma-Aldrich), MIRA-1 (Santa Cruz Biotechnology), Nutlin-3 (EMD Millipore), and NSC319726 (Selleck Chemicals).

### Cell Viability Assay

Cell viability was determined by the Sulforhodamine B Based In Vitro Toxicology Assay Kit (Sigma-Aldrich). Cells were plated in six-well plates, and after reaching 60%–70% confluency the cells were treated with chemicals at concentrations and hours indicated in the figures and figure legends. Staining and quantitative analysis were performed according to the manufacturer's method. All experiments were performed in duplicate.

### Total RNA Extraction and Quantitative Real-Time PCR Analysis

Total RNA was extracted using a Qiagen RNA extraction kit, converted to cDNA using an iScript cDNA Synthesis Kit (Bio-Rad), and analyzed by quantitative PCR (qPCR) using gene-specific primers. Primer sequences used were as follows: *p21* (forward: GGCGGCAGACCAGCATGACAGATT; reverse: GCAGGGGGCGCCAGGGTAT), *PUMA* (forward: GACCTCAACGCACAGTACGAG; reverse: AGGAGTCCCATGATGAGATTGT), *MDM2* (forward: GAATCATCGGACTCAGGTACATC; reverse: TCTGTCTCACTAATTGCTCTCCT), and *36B4* (forward: CAGATTGGCTACCCAAGTGT; reverse: GGGAGGGTGAATCCGTCTCC). qPCR was performed using an iCycler iQ5 real-time detection system (Bio-Rad) with LightCycler 480 SYBR Green I Master (Roche) according to the manufacturer's instructions. The quantitative value was normalized by *36B4* expression. All experiments were performed in triplicate.

### Immunoblotting

Cells were lysed with 1% Triton X-100 lysis buffer (20 mM Tris-HCl [pH 7.4], 5 mM EDTA, 10 mM Na<sub>4</sub>P<sub>2</sub>O<sub>7</sub>, 100 mM NaF, 2 mM Na<sub>3</sub>VO<sub>4</sub>, and 1% Triton X-100) supplemented with protease inhibitor cocktail (Roche). An equal

amount of total cellular proteins per sample was subjected to SDS-PAGE and transferred to a nitrocellulose membrane (Bio-Rad). Antibodies for immunoblotting included anti-p53 (DO-1; Santa Cruz), p21 (Cell Signaling Technology), PUMA (Cell Signaling), MDM2 (Calbiochem), Noxa (Calbiochem), Hsp40 (Santa Cruz), Hsp90 (Enzo Life Sciences), and  $\beta$ -actin (Sigma). Bands were detected using Western Lightning Plus ECL (PerkinElmer) or SuperSignal West Femto Maximum Sensitivity Substrate (Thermo Scientific). All experiments were performed independently at a minimum of three times.

### siRNA and shRNA Experiments

Vectors expressing shRNAs (pLKO.1-shLuc and pLKO.1-shp53 [TRCN0000003753, Sigma-Aldrich]) and small interfering RNAs (siRNAs) (siControl [12935-499, Invitrogen], sip53 [VHS40367, Invitrogen], siHsp40 [DNAJB1, Santa Cruz]) were used. All shRNA and siRNA constructs were introduced into cells by transfection with Lipofectamine 2000 or 3000 (Invitrogen) and Lipofectamine RNAiMax (Invitrogen), respectively, according to the manufacturer's protocol.

### Chromatin Immunoprecipitation

Cells were seeded in 10-cm dishes and began treatment of compound at 70% confluency for 6 hr. Cells were harvested and ChIP was carried out according to the manufacturer's instructions using a Chromatin Immunoprecipitation Assay Kit (EMD Millipore). Immunoprecipitation was performed at 4°C overnight with anti-p53 antibody (DO-1; Santa Cruz). qPCR amplifications were carried out using the following specific primers: *p21* (forward: CTCACATCCTCCTTCTCAG; reverse: CACACACAGAATCTGACTCCC), *PUMA* (forward: GCGAGACTGTGGCCTTGTGT; reverse: CGTCCAGGGTCCACA AAGT), and *MDM2* (forward: GGTTGACTCAGCTTTTCTCTTGT; reverse: GGA AAATGCATGGTTAAATAGCC). The amount of co-precipitating DNA was normalized to inputs. All experiments were performed in triplicate.

### Co-immunoprecipitation and Mass Spectrometry

Immunoprecipitation was performed as previously described (Namba et al., 2013) with modifications. In brief, cells were washed with PBS and incubated with PBS containing 1 mM diethylenetriaminepentaacetic acid (DTPA; Thermo Scientific) for 30 min at room temperature. The reaction was then quenched by 10 mM Tris (pH 7.5) for 15 min at room temperature. Cells were lysed with 0.5% Triton X-100 lysis buffer (20 mM Tris-HCl [pH 7.4], 5 mM EDTA, 10 mM Na<sub>4</sub>P<sub>2</sub>O<sub>7</sub>, 100 mM NaF, 2 mM Na<sub>3</sub>VO<sub>4</sub>, 0.5% Triton X-100) with protease inhibitor cocktail (Roche). Immunoprecipitation was performed using anti-p53 antibody (DO-1; Santa Cruz) with Protein A/G PLUS-Agarose (Santa Cruz) or agarose-conjugated anti-p53 antibody (DO-1 AC; Santa Cruz). Immunoprecipitated samples were subjected to mass spectrometry at the Taplin Biological Mass Spectrometry Facility of Harvard Medical School.

### Animal Experiments

All animal experiments were reviewed and approved by the Massachusetts General Hospital Subcommittee on Research Animal Care. For xenograft tumor models, cancer cell lines TOV-112D (5  $\times$  10<sup>6</sup> cells/mouse), CAL-33 (5  $\times$  10<sup>6</sup> cells/mouse), H1299 (1  $\times$  10<sup>7</sup> cells/mouse), and A431 (3  $\times$  10<sup>6</sup> cells/mouse) were injected subcutaneously into the flanks of nude mice (NCR nude, 5–6 weeks old). Tumor dimensions were measured, and volume was calculated by length (*L*) and width (*W*) using the formula (volume =  $\pi/6 \times L \times W^2$ ). Tumors were allowed to grow to 50 mm<sup>3</sup> prior to intraperitoneal injection of CTM at 1 mg/kg for days indicated in the figures and figure legends. Numbers of mice examined are as follows: TOV-112D (DMSO control: *n* = 7 and CTM-treated: *n* = 6), CAL-33 (DMSO control: *n* = 9 and CTM-treated: *n* = 9), A431 (DMSO control: *n* = 6 and CTM-treated: *n* = 6), and H1299 (DMSO control: *n* = 8 and CTM-treated: *n* = 8).

### Recombinant Proteins

Full-length WT p53 and p53 R175H were subcloned into pGEX-6P-1 vector. Full-length Hsp40 (DNAJB1) was subcloned into pET-28a vector. These bacterial expression constructs were used to transform *Escherichia coli* BL21 (New England Biolabs). Cells were induced with 0.05 mM isopropylthiogalactoside at 25°C for 24 hr. Recombinant proteins of interest were bound to GST beads (glutathione Sepharose 4B; GE Healthcare) or His beads (TALON Metal

Affinity Resin; Clontech). GST-R175H was incubated with PreScission Protease (GE Healthcare) to purify full-length p53 proteins.

### Biacore Assay and Analysis

Hsp40, mt p53 R175H, or Hsp70 was immobilized on CM5 sensor chip by amine coupling, and compound binding was assayed through a Biacore 3000 SPR system (GE Healthcare). CM5 sensor chips were coated with each of the purified proteins to a final resonance value of 1,000–2,000 response units. Various concentrations of compound in binding buffer (100  $\mu$ g/ml BSA, 0.01% Triton X-100, 2% DMSO in PBS [pH 7.4]) were injected for 90 or 180 s at a flow rate of 40  $\mu$ l/min, and each series of experiments was tested in duplicate. Sensorgram analyses were carried out using BIAevaluation software (GE Healthcare). All of the experiments were performed in duplicate.

### In Vitro Binding and Pull-Down Assay

In vitro binding assay was performed as previously described (King et al., 2001; Takada et al., 2012) with some modifications. In brief, purified recombinant p53 R175H (250 nM) or His-p53 R175H (55 nM, Thermo Scientific) and His-Hsp40 (1  $\mu$ M) in 90  $\mu$ l of assay buffer (PBS [pH 7.4], BSA [100  $\mu$ g/ml], 0.01% Triton X-100) with protease inhibitor cocktail (Roche) were incubated with the indicated concentrations of CTM in 10  $\mu$ l of DMSO at 4°C overnight. Subsequently, 900  $\mu$ l of binding buffer and p53 antibody (DO-1; Santa Cruz) with Protein A/G PLUS-Agarose (Santa Cruz) were added, followed by immunoprecipitation. All experiments were performed independently at a minimum of three times.

### Statistical Analysis

Statistical analysis was performed with GraphPad Prism 6 Software using Student's t test.

### SUPPLEMENTAL INFORMATION

Supplemental Information includes Supplemental Experimental Procedures, six figures, and five tables and can be found with this article online at <http://dx.doi.org/10.1016/j.chembiol.2015.07.016>.

### AUTHOR CONTRIBUTIONS

M.H., S.Y.H., and S.C. performed experiments, analyzed the experimental data, and wrote the manuscript. S.C. and T.R.R. fractionated the fungal extracts and identified CTM. S.B., K.W.Y., J.H.L., K.C., A.U.G., J.Z., and T.N. performed some of the critical experiments. V.K., D.J.N., and A.M. helped with high-throughput screening and analyzed the data. M.E.M. helped with research design. A.M., J.C., and S.W.L. designed experiments, analyzed the data, and co-wrote the paper, which was reviewed by all authors.

### ACKNOWLEDGMENTS

We thank Z. Yuan for MEF cells, X. Chen and J. Manfredi for mutant p53 plasmids and tet-inducible cell lines, J. Manfredi for p53 binding site of PUMA promoter plasmid, M. Taipale and S. Lindquist for materials and help on some heat-shock protein activity experiments, H. Li and S.J. Lee for help on Biacore studies, and W. Gu for in vitro gel-shift experiments. M.H. and T.N. were supported by postdoctoral fellowships for research abroad from the Japan Society for the Promotion of Science. M.H. was also supported by a research fellowship for research abroad from the Uehara Memorial Foundation. T.R.R. was supported by an F32 postdoctoral fellowship from the NIH (GM108415). The research was supported by NIH grants CA142805, CA149477, CA80058, and GM086258. Quantum-chemical calculations were run on the Odyssey cluster supported by the FAS Division of Science, Research Computing group at Harvard University.

Received: March 25, 2015

Revised: June 26, 2015

Accepted: July 8, 2015

Published: August 27, 2015

### REFERENCES

- Allen, M.A., Andrysiak, Z., Dengler, V.L., Mellert, H.S., Guarnieri, A., Freeman, J.A., Sullivan, K.D., Galbraith, M.D., Luo, X., Kraus, W.L., et al. (2014). Global analysis of p53-regulated transcription identifies its direct targets and unexpected regulatory mechanisms. *Elife* 3, e02200.
- Avantaggiati, M.L., Ogryzko, V., Gardner, K., Giordano, A., Levine, A.S., and Kelly, K. (1997). Recruitment of p300/CBP in p53-dependent signal pathways. *Cell* 89, 1175–1184.
- Bates, G.J., Nicol, S.M., Wilson, B.J., Jacobs, A.M., Bourdon, J.C., Wardrop, J., Gregory, D.J., Lane, D.P., Perkins, N.D., and Fuller-Pace, F.V. (2005). The DEAD box protein p68: a novel transcriptional coactivator of the p53 tumour suppressor. *EMBO J.* 24, 543–553.
- Bullock, A.N., and Fersht, A.R. (2001). Rescuing the function of mutant p53. *Nat. Rev. Cancer* 1, 68–76.
- Bunz, F., Dutriaux, A., Lengauer, C., Waldman, T., Zhou, S., Brown, J.P., Sedivy, J.M., Kinzler, K.W., and Vogelstein, B. (1998). Requirement for p53 and p21 to sustain G2 arrest after DNA damage. *Science* 282, 1497–1501.
- Bykov, V.J., Issaeva, N., Shilov, A., Hultcrantz, M., Pugacheva, E., Chumakov, P., Bergman, J., Wiman, K.G., and Selivanova, G. (2002). Restoration of the tumor suppressor function to mutant p53 by a low-molecular-weight compound. *Nat. Med.* 8, 282–288.
- Bykov, V.J., Issaeva, N., Zache, N., Shilov, A., Hultcrantz, M., Bergman, J., Selivanova, G., and Wiman, K.G. (2005). Reactivation of mutant p53 and induction of apoptosis in human tumor cells by maleimide analogs. *J. Biol. Chem.* 280, 30384–30391.
- Chai, J.-D., and Head-Gordon, M. (2008). Long-range corrected hybrid density functionals with damped atom-atom dispersion corrections. *Phys. Chem. Chem. Phys.* 10, 6615–6620.
- Chen, F., Wang, W., and El-Deiry, W.S. (2010). Current strategies to target p53 in cancer. *Biochem. Pharmacol.* 80, 724–730.
- Cherblanc, F., Lo, Y.P., De Gussem, E., Alcazar-Fuoli, L., Bignell, E., He, Y., Chapman-Rothe, N., Bultinck, P., Herrebout, W.A., Brown, R., et al. (2011). On the determination of the stereochemistry of semisynthetic natural product analogues using chiroptical spectroscopy: desulfurization of epidithiodioxopiperazine fungal metabolites. *Chem. Eur. J.* 17, 11868–11875.
- Cook, K.M., Hilton, S.T., Mecinovic, J., Motherwell, W.B., Figg, W.D., and Schofield, C.J. (2009). Epidithiodiketopiperazines block the interaction between hypoxia-inducible factor-1 $\alpha$  (HIF-1 $\alpha$ ) and p300 by a zinc ejection mechanism. *J. Biol. Chem.* 284, 26831–26838.
- Foster, B.A., Coffey, H.A., Morin, M.J., and Rastinejad, F. (1999). Pharmacological rescue of mutant p53 conformation and function. *Science* 286, 2507–2510.
- Fujimoto, H., Megumi, S., Okuyama, E., and Ishibashi, M. (2004). Immunomodulatory constituents from an ascomycete, *Chaetomium seminudum*. *J. Nat. Prod.* 67, 98–102.
- Gaiddon, C., Lokshin, M., Ahn, J., Zhang, T., and Prives, C. (2001). A subset of tumor-derived mutant forms of p53 down-regulate p63 and p73 through a direct interaction with the p53 core domain. *Mol. Cell. Biol.* 21, 1874–1887.
- He, T.C., Zhou, S., da Costa, L.T., Yu, J., Kinzler, K.W., and Vogelstein, B. (1998). A simplified system for generating recombinant adenoviruses. *Proc. Natl. Acad. Sci. USA* 95, 2509–2514.
- Hoe, K.K., Verma, C.S., and Lane, D.P. (2014). Drugging the p53 pathway: understanding the route to clinical efficacy. *Nat. Rev. Drug Discov.* 13, 217–236.
- Hong, B., Prabhu, V.V., Zhang, S., van den Heuvel, A.P., Dicker, D.T., Kopelovich, L., and El-Deiry, W.S. (2014). Prodigiosin rescues deficient p53 signaling and antitumor effects via upregulating p73 and disrupting its interaction with mutant p53. *Cancer Res.* 74, 1153–1165.
- Joerger, A.C., and Fersht, A.R. (2008). Structural biology of the tumor suppressor p53. *Annu. Rev. Biochem.* 77, 557–582.
- Kessler, J., Hahnel, A., Wichmann, H., Rot, S., Kappler, M., Bache, M., and Vordermark, D. (2010). HIF-1 $\alpha$  inhibition by siRNA or chetomin in human malignant glioma cells: effects on hypoxic radioresistance and monitoring via CA9 expression. *BMC Cancer* 10, 605.

- King, F.W., Wawrzynow, A., Hohfeld, J., and Zyllicz, M. (2001). Co-chaperones Bag-1, Hop and Hsp40 regulate Hsc70 and Hsp90 interactions with wild-type or mutant p53. *EMBO J.* 20, 6297–6305.
- Kung, A.L., Zabludoff, S.D., France, D.S., Freedman, S.J., Tanner, E.A., Vieira, A., Cornell-Kennon, S., Lee, J., Wang, B., Wang, J., et al. (2004). Small molecule blockade of transcriptional coactivation of the hypoxia-inducible factor pathway. *Cancer Cell* 6, 33–43.
- Lane, D.P. (1992). Cancer. p53, guardian of the genome. *Nature* 358, 15–16.
- Lawrence, M.S., Stojanov, P., Mermel, C.H., Robinson, J.T., Garraway, L.A., Golub, T.R., Meyerson, M., Gabriel, S.B., Lander, E.S., and Getz, G. (2014). Discovery and saturation analysis of cancer genes across 21 tumour types. *Nature* 505, 495–501.
- Lee, D., Kim, J.W., Seo, T., Hwang, S.G., Choi, E.J., and Choe, J. (2002). SWI/SNF complex interacts with tumor suppressor p53 and is necessary for the activation of p53-mediated transcription. *J. Biol. Chem.* 277, 22330–22337.
- Leroy, B., Fournier, J.L., Ishioka, C., Monti, P., Inga, A., Fronza, G., and Soussi, T. (2013). The TP53 website: an integrative resource centre for the TP53 mutation database and TP53 mutant analysis. *Nucleic Acids Res.* 41, D962–D969.
- Levine, A.J., and Oren, M. (2009). The first 30 years of p53: growing ever more complex. *Nat. Rev. Cancer* 9, 749–758.
- Mandinova, A., and Lee, S.W. (2011). The p53 pathway as a target in cancer therapeutics: obstacles and promise. *Sci. Transl. Med.* 3, 64rv61.
- Muller, P.A., and Vousden, K.H. (2014). Mutant p53 in cancer: new functions and therapeutic opportunities. *Cancer Cell* 25, 304–317.
- Murray-Zmijewski, F., Lane, D.P., and Bourdon, J.C. (2006). p53/p63/p73 isoforms: an orchestra of isoforms to harmonise cell differentiation and response to stress. *Cell Death Differ.* 13, 962–972.
- Namba, T., Tian, F., Chu, K., Hwang, S.Y., Yoon, K.W., Byun, S., Hiraki, M., Mandinova, A., and Lee, S.W. (2013). CDIP1-BAP31 complex transduces apoptotic signals from endoplasmic reticulum to mitochondria under endoplasmic reticulum stress. *Cell Rep.* 5, 331–339.
- Okamoto, T., Izumi, H., Imamura, T., Takano, H., Ise, T., Uchiyama, T., Kuwano, M., and Kohno, K. (2000). Direct interaction of p53 with the Y-box binding protein, YB-1: a mechanism for regulation of human gene expression. *Oncogene* 19, 6194–6202.
- Raj, L., Ide, T., Gurkar, A.U., Foley, M., Schenone, M., Li, X., Tolliday, N.J., Golub, T.R., Carr, S.A., Shamji, A.F., et al. (2011). Selective killing of cancer cells by a small molecule targeting the stress response to ROS. *Nature* 475, 231–234.
- Rehman, A., Chahal, M.S., Tang, X., Bruce, J.E., Pommier, Y., and Daoud, S.S. (2005). Proteomic identification of heat shock protein 90 as a candidate target for p53 mutation reactivation by PRIMA-1 in breast cancer cells. *Breast Cancer Res.* 7, R765–R774.
- Rokaeus, N., Klein, G., Wiman, K.G., Szekely, L., and Mattsson, K. (2007). PRIMA-1(MET) induces nucleolar accumulation of mutant p53 and PML nuclear body-associated proteins. *Oncogene* 26, 982–992.
- Rosser, M.F.N., and Cyr, D.M. (2007). Do Hsp40s act as chaperones or co-chaperones?, Chapter 4 In *Networking of Chaperones by Co-Chaperones*, G.L. Blatch, ed. (Springer), pp. 38–51.
- Sjogren, S., Inganas, M., Norberg, T., Lindgren, A., Nordgren, H., Holmberg, L., and Bergh, J. (1996). The p53 gene in breast cancer: prognostic value of complementary DNA sequencing versus immunohistochemistry. *J. Natl. Cancer Inst.* 88, 173–182.
- Staab, A., Loeffler, J., Said, H.M., Diehlmann, D., Katzer, A., Beyer, M., Fleischer, M., Schwab, F., Baier, K., Einsele, H., et al. (2007). Effects of HIF-1 inhibition by chetomin on hypoxia-related transcription and radiosensitivity in HT 1080 human fibrosarcoma cells. *BMC Cancer* 7, 213.
- Stelzl, U., Worm, U., Lalowski, M., Haenig, C., Brembeck, F.H., Goehler, H., Stroedicke, M., Zenkner, M., Schoenherr, A., Koeppen, S., et al. (2005). A human protein-protein interaction network: a resource for annotating the proteome. *Cell* 122, 957–968.
- Sugito, K., Yamane, M., Hattori, H., Hayashi, Y., Tohno, I., Ueda, M., Tsuchida, N., and Ohtsuka, K. (1995). Interaction between hsp70 and hsp40, eukaryotic homologues of DnaK and DnaJ, in human cells expressing mutant-type p53. *FEBS Lett.* 358, 161–164.
- Takada, K., Zhu, D., Bird, G.H., Sukhdeo, K., Zhao, J.J., Mani, M., Lemieux, M., Carrasco, D.E., Ryan, J., Horst, D., et al. (2012). Targeted disruption of the BCL9/beta-catenin complex inhibits oncogenic Wnt signaling. *Sci. Transl. Med.* 4, 148ra117.
- Waksman, S.A., and Bugie, E. (1944). Chaetomin, a new antibiotic substance produced by *Chaetomium cochliodes*: I. Formation and properties. *J. Bacteriol.* 48, 527–530.
- Wassman, C.D., Baronio, R., Demir, O., Wallentine, B.D., Chen, C.K., Hall, L.V., Salehi, F., Lin, D.W., Chung, B.P., Hatfield, G.W., et al. (2013). Computational identification of a transiently open L1/S3 pocket for reactivation of mutant p53. *Nat. Commun.* 4, 1407.
- Willis, A., Jung, E.J., Wakefield, T., and Chen, X. (2004). Mutant p53 exerts a dominant negative effect by preventing wild-type p53 from binding to the promoter of its target genes. *Oncogene* 23, 2330–2338.
- Yu, J., Zhang, L., Hwang, P.M., Kinzler, K.W., and Vogelstein, B. (2001). PUMA induces the rapid apoptosis of colorectal cancer cells. *Mol. Cell* 7, 673–682.
- Yu, X., Vazquez, A., Levine, A.J., and Carpizo, D.R. (2012). Allele-specific p53 mutant reactivation. *Cancer Cell* 21, 614–625.
- Yuan, Z., Villagra, A., Peng, L., Coppola, D., Glozak, M., Sotomayor, E.M., Chen, J., Lane, W.S., and Seto, E. (2010). The ATDC (TRIM29) protein binds p53 and antagonizes p53-mediated functions. *Mol. Cell. Biol.* 30, 3004–3015.